Medical & Biological Engineering & Computing
https://doi.org/10.1007/s11517-017-1756-1

SPECIAL ISSUE – ORIGINAL ARTICLE

Modeling and development of screen-printed impedance biosensor for cytotoxicity studies of lung carcinoma cells

Ahmad Fairuzabadi Mohd Mansor[1] · Irmanisha Ibrahim[2] · Ahmad Anwar Zainuddin[1] · Ioana Voiculescu[3] · Anis Nurashikin Nordin[1]

Received: 28 January 2017 / Accepted: 20 November 2017

Abstract
Electrical cell-substrate impedance sensing (ECIS) is a powerful technique to monitor real-time cell behavior. In this study, an ECIS biosensor formed using two interdigitated electrode structures (IDEs) was used to monitor cell behavior and its response to toxicants. Three different sensors with varied electrode spacing were first modeled using COMSOL Multiphysics and then fabricated and tested. The silver/silver chloride IDEs were fabricated using a screen-printing technique and incorporated with polydimethylsiloxane (PDMS) cell culture wells. To study the effectiveness of the biosensor, A549 lung carcinoma cells were seeded in the culture wells together with collagen as an extracellular matrix (ECM) to promote cell attachment on electrodes. A549 cells were cultured in the chambers and impedance measurements were taken at 12-h intervals for 120 h. Cell index (CI) for both designs were calculated from the impedance measurement and plotted in comparison with the growth profile of the cells in T-flasks. To verify that the ECIS biosensor can also be used to study cell response to toxicants, the A549 cells were also treated with anti-cancer drug, paclitaxel, and its responses were monitored over 5 days. Both simulation and experimental results show better sensitivity for smaller spacing between electrodes.

Keywords Screen-printed biosensor · A549 · Paclitaxel · Silver/silver chloride electrode · ECIS

1 Introduction

Lung cancer is the leading malignancy in cancer-related deaths in Southeast Asia with a mortality rate of 95 deaths per hundred thousand people in 2012 [8]. It originates from epithelial cells of certain parts of the lung such as bronchioles or alveolus. The rapid growth and fast spreading ability of the cells make this type of cancer a life-threatening disease as the symptoms are normally displayed only during the middle or even late stages of the cancer. Most late-stage treatments involve drug infusion into patients in the form of chemotherapy. Current methods of determining chemotherapy doses are based on body surface area (BSA) of the patients. This formulation method neglects individual factors such as age, gender, metabolism, and genetics, which may influence the adsorption rate of the drugs. Consequently, excessive exposure to these toxic chemotherapy drugs will result in side effects from as mild as hair loss to the more severe, vital organ dysfunction [21, 29]. Personalized treatments can help achieve more efficiency with minimal side effects as shown by clinical studies [29].

The challenge today is to provide a low-cost personalized chemotherapy treatment method. One of the options to realize this is to monitor a patient's response to chemotherapy in vitro. Monitoring of cellular proliferation and viability processes was formerly done using cell-based assay method. This conventional method involves cell-counting using optical microscopy. In time, this technique was replaced by real-time,

✉ Anis Nurashikin Nordin
anisnn@iium.edu.my

[1] Department of Electrical and Computer Engineering, International Islamic University Malaysia, Kuala Lumpur, Malaysia

[2] Department of Biotechnology Engineering, International Islamic University Malaysia, Kuala Lumpur, Malaysia

[3] Department of Mechanical Engineering, School of Engineering, City College of New York, New York, NY, USA

Published online: 16 December 2017

non-invasive, and label-free biosensing techniques such as electric cell-substrate impedance sensing (ECIS), mass sensing, and optical light spectroscopy [11]. Monitoring of cell behaviors non-invasively has gained wide attention over the past decade. The concept of ECIS was pioneered by Giaever and Keese in 1984 and evolved to be the most stable and effective technique of measuring cultured cells on microelectrodes with real-time impedance monitoring [7, 19]. A low-frequency AC signal is supplied to the electrodes to measure the impedance change caused by the cells' behavior. As cells adhere and spread on the electrodes, their insulating plasma membranes impede the electrical current flow forcing it to flow underneath and between the cells. This constrained current path results in large changes in the measured impedance [9]. These variations can be numerically analyzed as have been reported in various cellular studies to monitor adhesion, proliferation and differentiation [6, 11, 14, 26, 27], cell migration [5, 12], and cytotoxicity [1, 17, 22, 25].

In this paper, the ECIS concept was applied to monitor adhesion, proliferation and death of A549 cells, and the apoptosis induced by toxicity of paclitaxel-treated A549 cells. We varied the distance between electrodes, which was reported to have effect on the sensitivity of the impedance biosensor [30].Our goal is to evaluate how spacing between electrodes affects sensitivity to cell index measurement. Electrodes with smaller spacing are expected to be more sensitive compared to larger spacing. Specifically, in this research, the objective is to study which sensor is the best for monitoring A549 cancer cells when exposed to toxicants. Finite element simulation using COMSOL Multiphysics as well as sets of experiments was conducted to support the hypothesis. The proposed sensor was formed using screen-printed silver/silver chloride electrodes on a glass substrate. A thin layer of collagen was coated on the electrodes to promote cellular adhesion on the electrode surface. Cell culture wells made of polydimethylsiloxane (PDMS) were attached on the electrodes and covered with another layer of PDMS to avoid contamination during experiments. The main advantages expected of the proposed device are it being low cost, requiring small volumes of samples and reagents, being portable, and can support simultaneous and instantaneous measurements. In this article, the effect of varying gap spacing between electrodes towards the accuracy of the cellular measurement will be further studied with reference to our previous work that was presented in ICIBEL 2015 and published in IFMBE proceedings.

The organization of the paper is as follows: Section II describes the modeling and simulation of the electrode design using COMSOL Multiphysics. Simulation results will be discussed together with the hypothesis of the experimental results. Section III discusses the material, experimental procedure, and overall data presentation of the experimental results. Section IV elaborates on the experimental data and discussion of the findings in this study.

2 Materials and methods

2.1 Experimental materials and method

2.1.1 Sensor fabrication

The main issue in adopting personalized chemotherapy treatment is as aforementioned the lack of low-cost methods and reproducibility for cell-based assays. This work proposes using screen-printing technology as a means of low-cost fabrication for biosensors. Sensor fabrication techniques and procedures were previously explained and reported in [17]. Screen printing machine, equipment, and frame of polyester with 150 threads/in. mesh with 10-μm emulsion thickness were obtained from Jujo Technology Resources. The conductive and biocompatible silver/silver chloride paste was obtained from The Gwent Group. Glass substrates were cleaned with ethanol and rinsed with purified water and placed under the design mesh. Ink paste was poured on the mesh and pressed using a squeegee. The ink deposited through the mesh onto the glass following the design. The ink was cured in a box oven at 80 °C for 25 min. This curing condition had been optimized to attain the highest conductivity together with the strongest adhesion of the electrode with the substrate. The culture well was made out of polydimethylsiloxane (PDMS) as the culture chamber of the cells. PDMS was weighed and mixed with curing agent to the ratio of 10:1 and left overnight to solidify in a closed container. Once hardened, the PDMS was cut to fit the electrode size, punched to make wells on top of the electrode, glued onto the glass using a liquid-form PDMS, and left for another night to dry and harden. Each glass slide comprises five individual sensors of similar design to allow for simultaneous testing. The fabricated biosensor is shown in Fig. 1a. The impedance of the simulated design is shown in Fig. 1b; meanwhile, detailed geometry and designs are portrayed in Fig. 1c. The fabricated biosensors were sterilized under UV light for a few hours in a biosafety cabinet before being introduced to and tested with the cells.

2.1.2 A549 cell culturing and sensor coating

A549 lung carcinoma cell lines (ATCC® CCL185™) were obtained from the American Type Culture Collection (ATCC, Manassas, VA, USA), maintained and cultured in Dulbecco's modified Eagle medium (DMEM; Gibco, Paisley, UK), and supplemented with 10% (*v*/*v*) heat-inactivated fetal bovine serum (FBS; Gibco). The cell culture media were renewed for every two or 3 days. The A549 cells were incubated under standard cell culture in CO_2 incubator at 37 °C in an atmosphere containing 5% carbon dioxide (CO_2). Around 5×10^3 cells/ml A549 cell lines were seeded into each well sensor prior to the experiment.

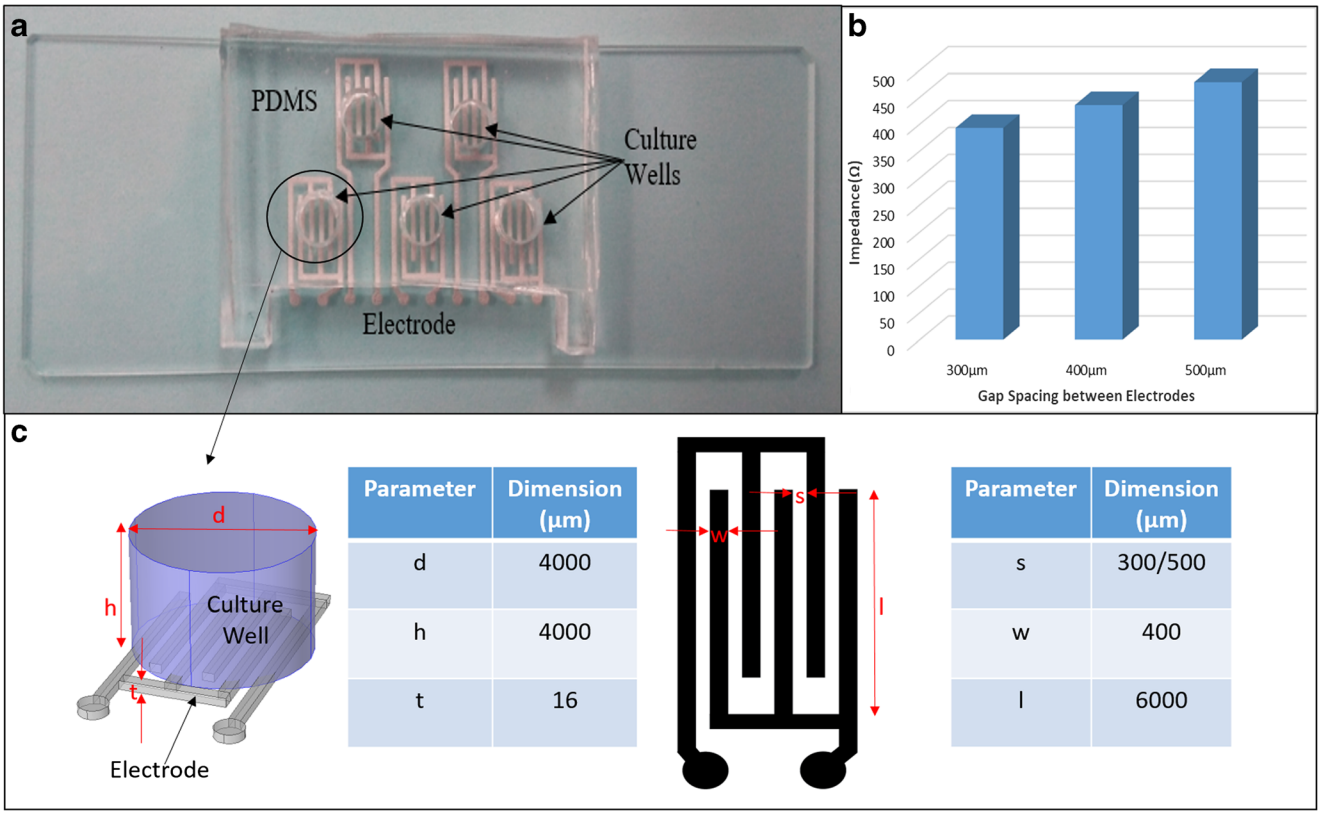

Parameter	Dimension (µm)
d	4000
h	4000
t	16

Parameter	Dimension (µm)
s	300/500
w	400
l	6000

Fig. 1 **a** The IDE sensors fabricated on glass slide: the culture chamber was made of PDMS and stuck on the electrode surface. **b** Impedance of simulated design: on the left is the smaller spacing between electrodes and on the right, the larger spacing between electrodes. **c** Design and geometric parameters of the fabricated culture wells and electrodes.

Collagen I, bovine (Gibco, UK) was diluted to 50 mg/L in 0.02-M acetic acid (Merck, Germany). The solution was added onto the biosensor at 200 µg per cm^2 and incubated for 2 hours. Excess collagen solution was carefully aspirated from the biosensor and rinsed with phosphate-buffer saline (PBS, Gibco) before inoculating the cells into the well.

2.1.3 Cytotoxicity test

The cells and drugs used in this study were well-documented non-small human lung cancer cells, A549 carcinoma cell line, and anti-cancer drug, paclitaxel (Gibco; Paisley, UK), respectively. Paclitaxel or Taxol is a chemotherapy drug used for treating solid tumor cancers. Paclitaxel interferes with the microtubule dynamics of the cells, prohibiting cell cycle progression by inhibiting the function of mitotic spindle and inducing apoptosis of the treated cells [10, 15]. Goncalves et al. [10] investigated the influence of Taxol on A549 cellular microtubule dynamics using immunofluorescence microscopy technique. A low concentration of Taxol was inoculated and reported to decrease the shortening rate and length but increases the time pause reflecting the stability of the overall microtubule dynamics.

The final concentration of Taxol with IC_{50} value of 0.857 µg/ml was inoculated immediately with the cell suspension prior to cell seeding and cell culture on the electrodes [3]. The response of the cells to the drugs was observed using the fabricated sensor.

2.1.4 Cell viability assay

Prior to biosensor test, 5×10^3 cells/ml A549 cell lines were seeded and cultured into ten T25-flasks to monitor the growth trend of the cells. Every 12 h, a flask was taken out of the incubator for cell counting using conventional technique for a total duration of 120 h. Cells were detached from the flask and stained using trypan blue dye in a 1:1 ratio of 5 µL. Cell counting was done using a hemocytometer and observed under an optical microscope. This procedure was repeated for three times to reach an average number of viable cells for the growth trend plot.

2.2 Theoretical and finite element analysis for the sensor

2.2.1 Electrode structure

Planar interdigitated electrode structures (IDEs) have shown improved sensitivity in the detection of impedance variation as compared to circular monoplanar structure [16]. IDEs have

been configured such that it consists of repetitive electrode patterns in order to obtain a strong signal with similar principals as that of parallel plate capacitors. Ideally, an electric field will be generated between the two parallel plates of positive and negative terminals, penetrating the test sample resulting in impedance changes [13, 20]. Different levels of electric field excitation will be generated with respect to the different spacing between adjacent electrodes [23]. The analysis on different spacing between electrodes to the level of magnitude of electric field and impedance will be carried out using COMSOL Multiphysics.

2.2.2 Modeling of interdigitated electrode structures in COMSOL

COMSOL Multiphysics is a finite element method software platform for modeling and simulating multiple physics applications using numerical techniques. For the purpose of simulation, the AC/DC module was selected. The application was in 3D mode and electric currents interface was used to simulate the electric field of the design. The simulation was conducted with the assumption of negligible inductive effect of the system and purely capacitive effect based on the parallel plate.

Two identical electrodes (working and counter) with width of 400 μm, length of 6000 μm, and thickness of 16 μm [28] were designed with different spacing between electrodes of 300, 400, and 500 μm. A cylinder with dimensions of 5000-μm radius and 4000-μm height, defined as Dulbecco modified Eagle media (DMEM), was designated on top of the electrodes as the test sample to replicate the actual design of the sensor for simulation purposes. DMEM electrical conductivity and relative permittivity were set to1.38 S/m and 80, respectively [2, 6]. Silver was chosen as the electrode metal, where its parameters are predefined in COMSOL's library.

Appropriate boundary conditions were applied to the simulation model. A ground potential boundary condition was applied to the counter electrode and a terminal with voltage condition was assigned to the working electrode. This is to generate electric currents from the working electrode to the counter electrode, hence the electric field. The module performs numerical calculations based on Ohm's law as in Eq. (1):

$$J = \sigma E + j\omega D + J_e \tag{1}$$

where J is the current density, σ is the conductivity of DMEM, E is the electric field, D is the electric displacement, and J_e is the external current density. However, since no external current density was defined, the equation can further be expressed as

$$J = \sigma E + j\omega D \tag{2}$$

This equation will be used to determine the impedance of the simulation. The electric field (E) and electric displacement (D) were obtained from the gradient of voltage (V) at each static point as in Eqs. (3) and (4):

$$E = -\nabla V \tag{3}$$

$$D = \varepsilon_o \varepsilon_r E \tag{4}$$

ε_o and ε_r are the permittivity of free space and permittivity of the electrode, respectively. For the impedance, the equation is predefined as the ratio of voltage to total current at the electrode and is automatically computed by the terminal feature as the inverse of admittance. Default fine tetrahedral element mesh was chosen for this simulation.

2.2.3 Relationship between electrode spacing and cell index

Cell index (CI) is a dimensionless representation method for cells' adhesion status on electrode, derived from the impedance measurement used by commercialized products such as RT-CES and xCELLigence system [4]. CI can be calculated based on the following Eq. (5):

$$\mathrm{CI} = \max_{i=1,..n}\left[\frac{R_{cell}(f_i)}{R_b(f_i)} - 1\right] \tag{5}$$

where R_b indicates the frequency-dependent resistance of the media, and R_{cell} indicates the frequency-dependent resistance of the cells. In this study, electric field is a crucial parameter in determining the sensitivity of the design. In parallel plate systems, electric field E can be derived as in (6):

$$E = \frac{V}{d} \tag{6}$$

where V is the voltage applied and d is the spacing between electrodes. Resistance of cells on the other hand can be defined as in (7):

$$R_{cell} = \frac{\rho_{cell} T}{A} \tag{7}$$

where ρ_{cell} is the resistivity of the cancer cells, T is the thickness of the cell layer, and A is the total electrode surface area. Substituting (6) and (7) into the current density equation based on Ohm's law will result in a derivation as shown in (8)

$$R_{cell} = \frac{R_{total} T}{d} \tag{8}$$

Replacing (8) into (5) will lead to the final equation of (9)

$$\mathrm{CI} = \frac{T}{d - T} \tag{9}$$

with parameters T as the thickness of the cell layer and d as the distance between the electrodes. The final equation suggests that the cell index has an inversely proportional relationship with the spacing between electrodes. A smaller spacing is expected to have a higher cell index compared to larger spacing given that cell density, environment, and types of cell are constant parameters. Nevertheless, these derivations assumed that the current flows radially between the ventral surfaces of the cell, without current penetration through the cells due to low frequency.

2.2.4 Impedance measurement with biosensor

The impedance measurements were performed by applying AC signals with peak amplitude of 500 mV onto the working electrode. The impedance response was manually measured on the outer electrodes for every 12 h up to 120 h by using the Agilent precision impedance analyzer 4294A. The frequency of interest was the lowest, i.e., 40 Hz to avoid any detrimental effects on the cells by higher frequencies. The measurements were in terms of impedance value (Z) and phase angle (θ). The data was analyzed and calculated to plot the cell index number.

2.2.5 Impedance to cell index

Since the measurements taken from the impedance analyzer were in the form of impedance and phase, CI can be calculated based on Eqs. (10) and (11) below [17].

$$|Z| = \sqrt{R^2 + X^2} \tag{10}$$

$$\theta = \tan^{-1}\left(\frac{X}{R}\right) \tag{11}$$

The impedance (Z) and phase (θ) values obtained from experimental measurements can be further derived into resistance (R) and reactance (X). When low frequency electrical signal is applied, presence of cells will restrict current flows as current cannot flow through the cell membranes. During this period, cellular behavior will be represented by the resistive element. Basically, CI is the ratio of cell impedance with respect to control impedance. Control impedance is the impedance of the system without the cells. Theoretically, CI will become zero when there are no cells attached to the electrodes. A higher CI indicates a higher number of cells adhering onto the electrodes. Any changes in cell adherence and morphology can be detected by measuring the changes, either increase or decrease of CI.

3 Results and discussion

3.1 Simulation results

The simulation was executed by applying periodic signals with amplitude of 0.5 V, at 40 Hz, to the working electrode. The magnitude of electric field on the surface of the working electrode was plotted on a graph shown in Fig. 2 for all spacings—300, 400, and 500 μm. A higher magnitude of electric field can be seen from the 300-μm spacing, in comparison of the other two. This simulation agreed with theory [20], of which weaker electric field is generated at higher spacing between electrodes.

Based on the electric field results generated from the simulation, the smaller spacing between electrodes was expected to be more sensitive compared to that of the larger spacing. Although the impedance is lower, the presence of higher magnitude field on the electrode would have made it more sensitive in cellular studies applications. During cell culture, cells will adhere and spread on the surface of the electrodes, which apply to both sensors. A higher magnitude of electric field on the sensing area would result in higher current density in that particular area. This would also affect the total current flowing through the electric field based on Maxwell's equation given in (12)

$$I = \int J.dS \tag{12}$$

Therefore, it can be concluded that the total current flow will increase proportionally to the electric field. The relation between these two variables can be simplified as in Eq. (13):

$$I = \int J.E\ (\sigma + \varepsilon_0 \varepsilon_r) \tag{13}$$

where

I is the total current flowing inside the sensor.
J is the current density.
E is the electric field.
σ is the conductance of the culture media.
ε_0 is the permittivity of free space.
ε_r is the permittivity of the culture media.

During cell culture, cells will adhere and spread on the surface of the electrodes for both sensors, with a gap of 10–20 nm between the cell-electrode surfaces. At low frequencies, the cells have poor conductance and they restrict electric fields from penetrating the cells. This results in an increase in impedance values. Currents are forced to bypass the cells through the small junction in between the cell membranes and the cell-electrode interface. Higher total current would result in better sensitivity measurement as higher amount of current produced can be allocated per unit cell. Considering the surface areas are constant for all spacing, an assumption was made such that the total cells adhered are approximately

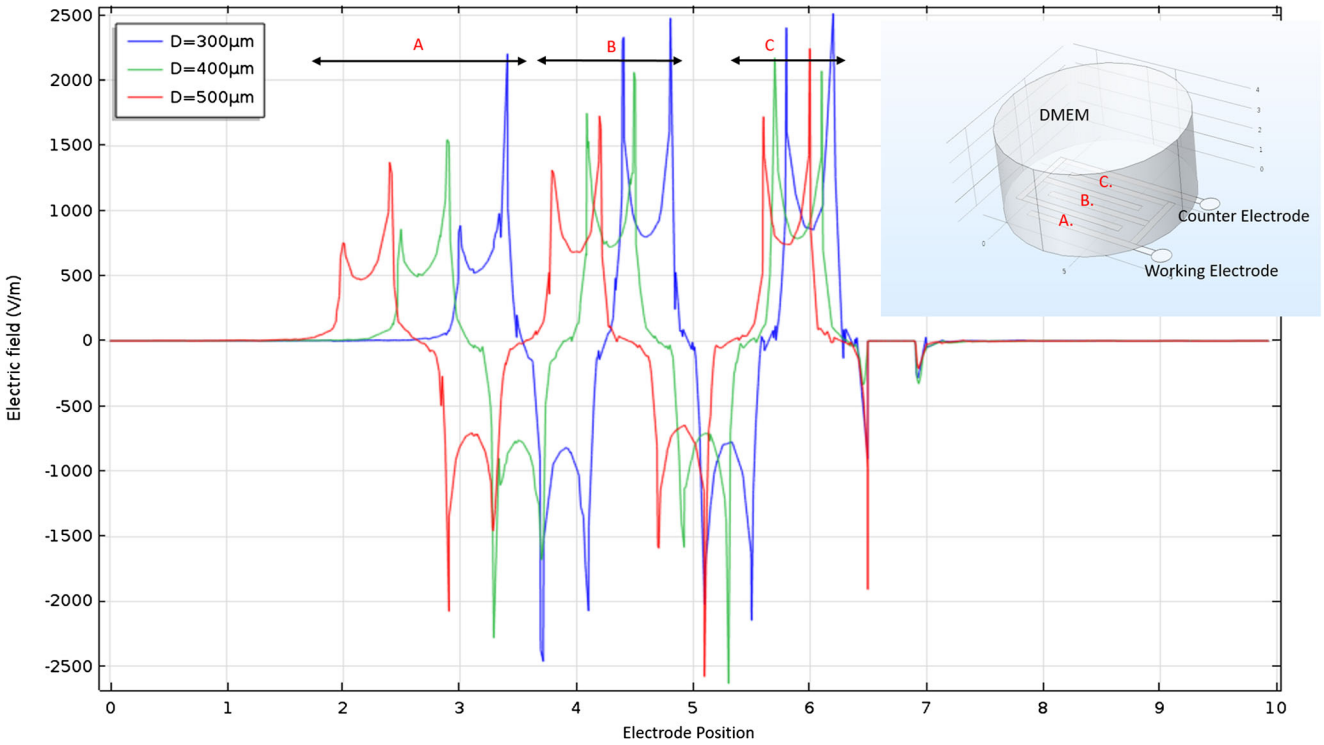

Fig. 2 Electric field magnitude on the surface of electrode versus the electrode position. A, B, and C represent the location of each finger of the working electrode in the graph. Higher magnitude of electric field is seen in sensors with lower spacing between electrodes. This magnitude ranges approximately 100–200 V/m higher in sensors with 300-µm spacing. Inset diagram: 3D geometry used for simulation of the different spacing between electrodes

the same for all cases. This theory will be tested experimentally using the A549 carcinoma cells in the next experiment section.

3.2 Experimental results

3.2.1 Cell index

Two sensors (A and B) with different IDE spacing were seeded with A549 cells and their impedance measurements were recorded every 12 h for 6 days. The measurements were quintuplicate, meaning five sets of experiments were conducted at different times using different cell batches and plotted as the average of the CI measurement. The average impedance results of the CI measurement versus time were plotted as in Fig. 3.

As shown in Fig. 3, the cell growth cycle can be characterized into four phases: lag, log, stationary, and death [24]. The first cell cycle phase is the lag phase. During this phase, cells will try to adapt with the new surrounding environment. At the beginning of the experiment, cells were introduced and cultured inside the well of the biosensor. No changes concentration occurred during this period. However, as shown in the lag phase from time 12 to 24 h in Fig. 4, CI from the biosensors show a significant increase despite having no changes in cell concentrations. The impedance increase was due to the adherence of A549 cells on the electrode surface with the support of collagen as binding proteins. Adherence of cells on the electrode surface triggered an increment in impedance readings.

The log phase occurs between 24 to 96 h, where the cells undergo proliferation, division, and rapid multiplication. The graph suggests that the increasing concentration of cells is represented by the increasing CI. Several fluctuations of CI occurred between 24 to 60 h due to cell division. During cell division, a parent cell will split into two smaller daughter cells. Division causes a slight decrease in impedance as the process tends to expose the surface areas of the electrodes and in between cellular membranes that allow current to flow easily. The CI reached its peak at time of 96 h, similar to the maximum cell concentration obtained using conventional T-flask method.

For stationary and death phases, which occurred between 96 to 120 h, cell concentration began to decline indicating that the cells were undergoing the death stage. A similar decline trend curve was observed using the biosensors as with the conventional T-flask method. The CI showed a massive drop, resulting in lower impedance than the initial value of CI. This was due to the detachment of dead cells from the electrode surface. Since most of the adhered cells were no longer viable, they will slowly detach from the surface and become

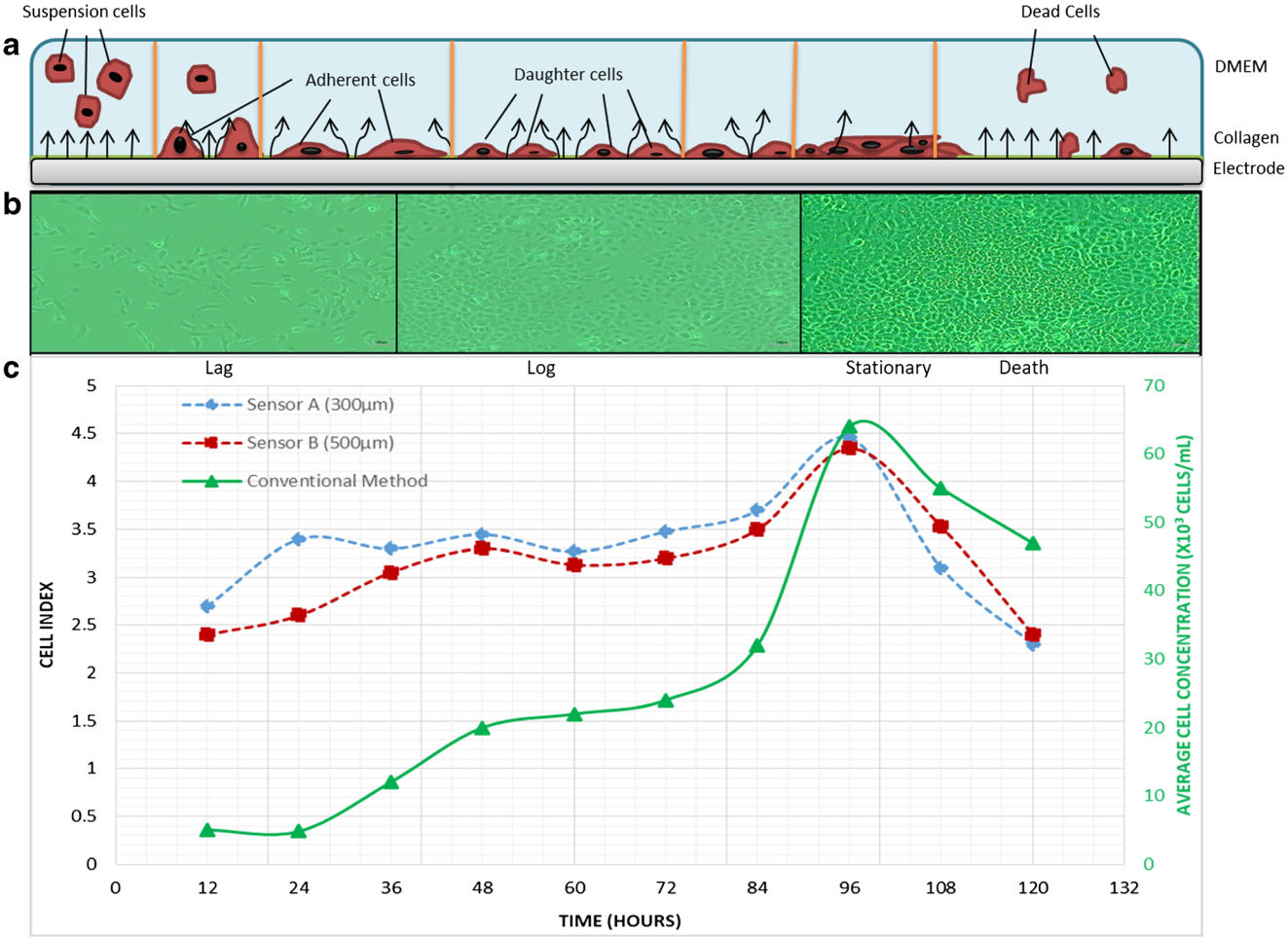

Fig. 3 Comparison of monitoring cellular growth using conventional method (cell counting under microscope) and impedance biosensor technique. **a** Illustration of biological event occurred on the sensor. The arrows indicate the flow of current. **b** Microscopic image inside the T-Flask taken at time 24, 60, and 96 h. The scale bar is in 100 µm. **c** The graph indicates the CI from impedance measurement and average cell concentration from cell counting procedure. Cell index on the right axis is the scale for sensors A and B, while the average cell concentration (green) axis on the right is the scale for the conventional method

suspended in the surroundings, leading to an increase in current flow from the electrodes to the surroundings.

3.2.2 Cell index response of paclitaxel-treated cells

Figure 4 plots cell index versus time for four different experiments, sensors A and B treated with Taxol and untreated sensors A and B or the control group. As seen in Fig. 4, both Taxol-treated sensors showed a decrease in CI values throughout the whole duration of the measurements compared to its initial values at 12 h. The nature of the drug prevents protein production required by the cells in mitosis or division process, thwarting its capability to multiply. Therefore, cells will end up dying a natural death by apoptosis. This explains the decreasing CI values over time as the adhered cells slowly die and detach from the electrodes. However, in a group of cancer cells, there are mixed combinations of drug-sensitive cells and drug-resistant cells [18]. Drug-sensitive cells can easily be penetrated by the drugs; however, drug-resistant cells require longer time or a different dosage to die. At low concentrations of Taxol (less than 10 nM), some cells can become drug-resistant cells. Therefore, some of the cells were still viable and proliferate as normal, causing CI to inconsistently increase several times during the toxicity test. The presence of drug-resistant cells explains the fluctuations in impedance readings. Based on these experiments, it can be concluded that this sensor is successful in monitoring the response of A549 when exposed to Taxol.

3.2.3 Sensitivity of the sensor

From the observed CI measurements for both experiments in Figs. 3 and 4, lower spacing between electrodes exhibits a higher number of CI compared to alternate configurations. The experimental results agree with the theory such that reduced spacing between electrodes tends to increase cell

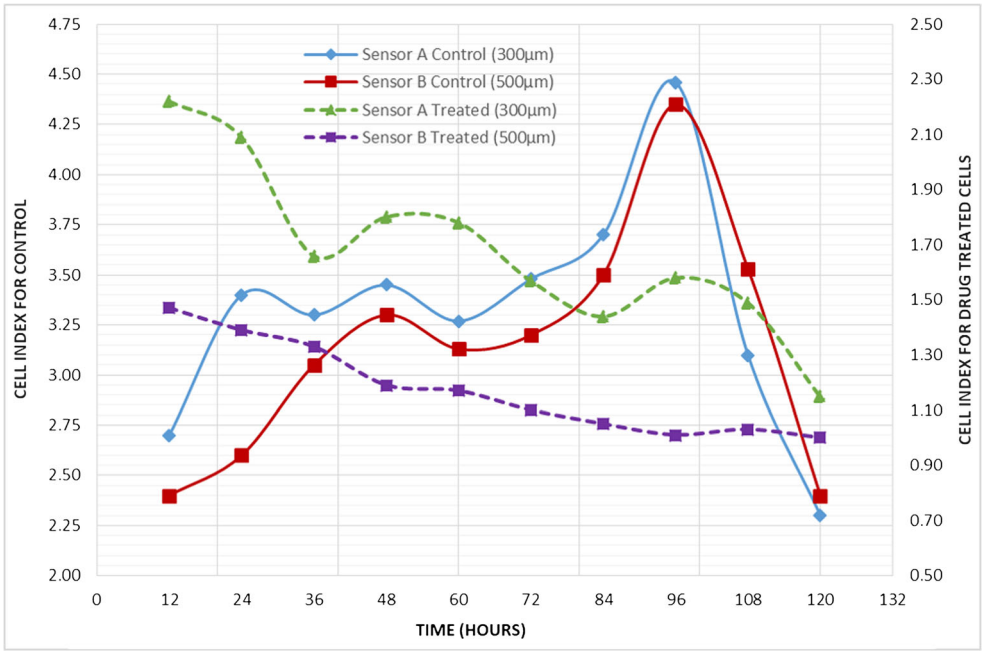

Fig. 4 Cell index of paclitaxel-treated A549 cells as compared to non-treated cells (control). Drugs were introduced at the beginning of the experiment

impedance-sensing performance. The magnitude of the electric field generated by the electrodes is proportional to the sensitivity of the sensor. Lower spacing between electrodes will increase the CI measurements by giving higher current density and better electrical representations of the cells.

4 Conclusion

In conclusion, we have fabricated a low-cost biosensor capable of characterizing cellular behavior of A549 cancer cells specifically when exposed to Taxol. In this paper, a study of two sensors with varied IDE spacings has been accomplished through both means of simulation and experiment in order to optimize the sensitivity of the design. The results have indicated that smaller spacing between electrodes exhibits higher sensitivity for the two designs. It can be concluded that this biosensor can be utilized to characterize cellular events and has potential to be adopted as low-cost biosensor for personalized drug screening sensor.

Funding information This work is supported by Malaysia Ministry of Science and Technology (MOSTI) e-Science Research Grant (SF16-004-0073) and Malaysia Ministry of Education FRGS Research Grant (FRGS14-111-0352).

References

1. Anh-Nguyen T, Tran D, Pliquett U, Urban G (2015) Behavior and the response of cancer cells on anticancer drug treatment monitored with microelectrode array. Procedia Eng 120:928–931. https://doi.org/10.1016/j.proeng.2015.08.801
2. Arnold WM, Fuhr G (1994) Increasing the permittivity and conductivity of cellular electromanipulation media. In: Industry Applications Society Annual Meeting, Conference Record of the 1994 IEEE. IEEE, p 1470–1476
3. Asphahani F, Zhang M (2007) Cellular impedance biosensors for drug screening and toxin detection. Analyst 132(9):835–841. https://doi.org/10.1039/b704513a
4. Boyd JM, Huang L, Xie L, Moe B, Gabos S, Li X-F (2008) A cell-microelectronic sensing technique for profiling cytotoxicity of chemicals. Anal Chim Acta 615(1):80–87. https://doi.org/10.1016/j.aca.2008.03.047
5. Chan C-M, Huang J-H, Chiang H-S, Wu W-B, Lin H-H, Hong J-Y, Hung C-F (2010) Effects of (−)-epigallocatechin gallate on RPE cell migration and adhesion. Mol Vis 16:586–595
6. Chen M-T, Jiang C, Vernier PT, Wu Y-H, Gundersen MA (2009) Two-dimensional nanosecond electric field mapping based on cell electropermeabilization. BMC Biophys 2:9
7. Cui Y, An Y, Jin T, Zhang F, He P (2017) Real-time monitoring of skin wound healing on nano-grooves topography using electric cell-substrate impedance sensing (ECIS). Sensors Actuators B Chem 250:461–468. https://doi.org/10.1016/j.snb.2017.04.183
8. Ferlay J, Soerjomataram I, Dikshit R, Eser S, Mathers C, Rebelo M, Parkin DM, Forman D, Bray F (2015) Cancer incidence and mortality worldwide: sources, methods and major patterns in GLOBOCAN 2012. Int J Cancer 136(5):E359–E386. https://doi.org/10.1002/ijc.29210
9. Giaever I, Keese CR (2012) Electric cell-substrate impedance sensing concept to commercialization. In: Jiang W (ed) Electric cell-substrate impedance sensing and cancer metastasis, vol 17. Springer, Dordrecht
10. Goncalves A, Braguer D, Kamath K, Martello L, Briand C, Horwitz S, Wilson L, Jordan M (2001) Resistance to Taxol in lung cancer cells associated with increased microtubule dynamics. Proc Natl Acad Sci 98(20):11737–11742. https://doi.org/10.1073/pnas.191388598
11. Hong J, Kandasamy K, Marimuthu M, Choi CS, Kim S (2011) Electrical cell-substrate impedance sensing as a non-invasive tool for cancer cell study. Analyst 136(2):237–245. https://doi.org/10.1039/C0AN00560F

12. Hsu C-C, Tsai W-C, Chen CP-C, Lu Y-M, Wang J-S (2010) Effects of negative pressures on epithelial tight junctions and migration in wound healing. Am J Phys Cell Phys 299(2):C528–C534. https://doi.org/10.1152/ajpcell.00504.2009
13. Jacobs P, Varlan A, Sansen W (1995) Design optimisation of planar electrolytic conductivity sensors. Med Biol Eng Comput 33:802–810
14. Janshoff A, Kunze A, Michaelis S, Heitmann V, Reiss B, Wegener J (2010) Cell adhesion monitoring using substrate-integrated sensors. J Adhes Sci Technol 24(13-14):2079–2104. https://doi.org/10.1163/016942410X507939
15. Kirkegaard J, Clausen CH, Rodriguez-Trujillo R, Svendsen WE (2014) Study of paclitaxel-treated HeLa cells by differential electrical impedance flow cytometry. Biosensors 4(3):257–272. https://doi.org/10.3390/bios4030257
16. Liu Q, Wang P (2009) Cell-based biosensors: principles and applications. Artech House, Norwood
17. Mansor A, Ibrahim I, Voiculescu I, Nordin A (2015) Screen printed impedance biosensor for cytotoxicity studies of lung carcinoma cells. In: Ibrahim F, Usman J, Mohktar M, Ahmad M (eds) International conference for innovation in biomedical engineering and life cciences. IFMBE Proceedings, vol 56. Springer, Singapore
18. Persidis A (1999) Cancer multidrug resistance. Nat Biotechnol 17(1):94–95. https://doi.org/10.1038/5289
19. Pradhan R, Rajput S, Mandal M, Mitra A, Das S (2014) Frequency dependent impedimetric cytotoxic evaluation of anticancer drug on breast cancer cell. Biosens Bioelectron 55:44–50. https://doi.org/10.1016/j.bios.2013.11.060
20. Rahman MSA, Mukhopadhyay SC, Yu P-L (2014) Novel planar interdigital sensors. In: Novel sensors for food inspection: modelling, fabrication and experimentation. Smart Sensors, Measurement and Instrumentation, vol 10. Springer, Cham
21. Rosenberger EE, English AE, Bose DD, Sani SN, Moy AB (2014) A multiplexed optical micro-impedance biosensor array for quantitaitive cancer drug assays. In: Bioengineering Conference (NEBEC), 2014 40th Annual Northeast. IEEE, p 1–2
22. Sun X, Ji J, Jiang D, Li X, Zhang Y, Li Z, Wu Y (2013) Development of a novel electrochemical sensor using pheochromocytoma cells and its assessment of acrylamide cytotoxicity. Biosens Bioelectron 44:122–126. https://doi.org/10.1016/j.bios.2013.01.031
23. Syaifudin AM, Mukhopadhyay SC, Yu P-L, Haji-Sheikh MJ, Chuang C-H, Vanderford JD, Huang Y-W (2011) Measurements and performance evaluation of novel interdigital sensors for different chemicals related to food poisoning. Sensors J IEEE 11:2957–2965
24. Todar K (2006) Todar's online textbook of bacteriology. University of Wisconsin-Madison Department of Bacteriology
25. Wang L, Wang H, Mitchelson K, Yu Z, Cheng J (2008) Analysis of the sensitivity and frequency characteristics of coplanar electrical cell–substrate impedance sensors. Biosens Bioelectron 24(1):14–21. https://doi.org/10.1016/j.bios.2008.03.018
26. Xu Y, Lv Y, Wang L, Xing W, Cheng J (2012) A microfluidic device with passive air-bubble valves for real-time measurement of dose-dependent drug cytotoxicity through impedance sensing. Biosens Bioelectron 32(1):300–304. https://doi.org/10.1016/j.bios.2011.12.009
27. Yu H, Wang J, Liu Q, Zhang W, Cai H, Wang P (2011) High spatial resolution impedance measurement of EIS sensors for light addressable cell adhesion monitoring. Biosens Bioelectron 26(6):2822–2827. https://doi.org/10.1016/j.bios.2010.08.032
28. Zainuddin AA, Mansor AFM, Rahim RA, Nordin AN (2017) Optimization of printing techniques for electrochemical biosensors. In: AIP Conference Proceedings, vol 1. AIP Publishing, Melville, p 020066
29. Zhang B, Wang R, Wang Y, Li Y (2013) A portable impedance biosensor for detection of multiple avian influenza viruses. In: SENSORS, 2013 IEEE. IEEE, Baltimore, p 1–4
30. Zou L, Wang Q, Tong M, Li H, Wang J, Hu N, Wang P (2016) Detection of diarrhetic shellfish poisoning toxins using high-sensitivity human cancer cell-based impedance biosensor. Sensors Actuators B Chem 222:205–212. https://doi.org/10.1016/j.snb.2015.08.061

Ahmad Fairuzabadi Mohd Mansor is a PhD candidate in International Islamic University Malaysia. He received his Bachelor's and Master's degree from Department of Electrical and Computer Engineering, International Islamic University Malaysia in 2013 and 2016, respectively. His research interests include electric cell-substrate impedance sensing (ECIS) technology, biosensor design, fabrication and application, and biosensing system design.

Irmanisha Ibrahim was a research assistant at Biotechnology Engineering Department, International Islamic University Malaysia. She has a degree in Biochemical-Biotechnology Engineering from International Islamic University Malaysia in 2011. Then, she obtained MS degree in Biotechnology Engineering from International Islamic University Malaysia in 2015. Her research area covers animal cell culture, toxicological test, printed electronics, and medical devices.

Ahmad Anwar Zainuddin is a PhD candidate in International Islamic University Malaysia He received his Bachelor's and Master's degree from Department of Electronic and Computer Engineering, International Islamic University Malaysia in 2011 and 2013, respectively. He worked as a RF-MEMS engineer in Silterra Malaysia in 2011, before he becomes a PhD candidate in International Islamic University Malaysia in 2015. His research interests include acoustic wave electrochemistry biosensors, computational mechanics, structural dynamics, smart materials and structures, and modeling of MEMS devices.

Ioana Voiculescu is an associate professor in the Mechanical Engineering Department, the City College of New York, New York. She received her PhD in Mechanical Engineering from the Technical University "Politehnica," Timisoara, Romania, and her ScD in Mechanical Engineering from the George Washington University, Washington, DC, in 2005. Since 2002, Dr. Voiculescu is a member of the ASME and IEEE. She published several journal papers in the area of microelectromechanical systems (MEMS) chemical and biological sensors.

Anis Nurashikin Nordin is an associate professor in Electronics Engineering Department, International Islamic University Malaysia. She has a BS degree in Computer and Information Engineering from International Islamic University Malaysia in 1999. She obtained both MS and PhD degrees in Computer Engineering from the George Washington University, Washington, DC, in 2002 and 2008, respectively. Her research area covers personalized healthcare devices, MEMS, BioMEMS, SAW devices, printed electronics, and microfluidics.